Physikalisch-Technische Bundesanstalt
National Metrology Institute

The following article is hosted by PTB.

DOI: 10.7795/810.20251001B
It is provided for personal use only.

Production of radioactive traceable reference materials for measuring radioactive pollutants in the environment

Acknowledgement:

The project 21GRD09 MetroPOEM has received funding from the European Partnership on Metrology, co-financed from the European Union's Horizon Europe Research and Innovation Programme and by the Participating States.

Funder name: European Partnership on Metrology

Funder ID: 10.13039/100019599

Grant number: 21GRD09 MetroPOEM

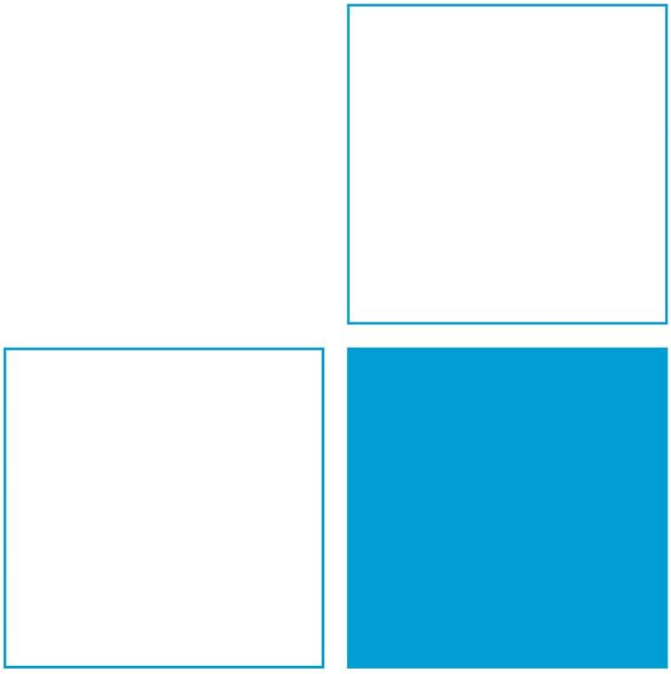

Originally published at:
10.1016/j.apradiso.2025.112204

License: CC-BY 4.0

Production of radioactive traceable reference materials for measuring radioactive pollutants in the environment

L. Chambon[1], S. Gupta[2], H. Isnard[2], S. Pierre[1], B. Sabot[1], D. Arnold[3], M. Christl[4], C. Cuer[1], J. Eberhardt[3], L. Flierl[3], S. Jerome[5], A. Lehnert[6], M. Mazánová[7], J.K. Nikolić[8], H. Pérez-Tribouillier[4], J. Qiao[9], B. Russell[10], C. Walther[6], V. Lourenço[1].

[1]Université Paris-Saclay, CEA, List, Laboratoire National Henri Becquerel (LNE-LNHB), 91120 Palaiseau, France (lucille.chambon@cea.fr and valerie.lourenco@cea.fr)

[2]Université Paris-Saclay, CEA, Service de Physico-Chimie (SPC), 91191 Gif sur Yvette, France (soumya.gupta@cea.fr and helene.isnard@cea.fr)

[3]Physikalisch-Technische Bundesanstalt, Bundesallee 100, 38116 Braunschweig, Germany (dirk.arnold@ptb.de, janine.eberhardt@ptb.de, lukas.flierl@ptb.de)

[4]Laboratory of Ion Beam Physics, Department of Physics, ETH Zürich, 8093 Zürich, Switzerland (hperez@phys.ethz.ch, mchristl@phys.ethz.ch)

[5]Norges miljø- og biovitenskapelige universitet, Elizabeth Stephansen vei 29, 1433 Ås, Norway (simon.mark.jerome@nmbu.no)

[6]Leibniz Universität Hannover, Herrenhäuser Straße 2, Gebäude 4113, 30419 Hannover, Germany (walther@irs.uni-hannover.de and lehnert@irs.uni-hannover.de)

[7]Czech Metrology Institute, Okruzni 31, Brno 63800, Czech Republic (mmazanova@cmi.cz)

[8]Vinča Institut za Nuklearne Nauke, Serbia (jnikolic@vin.bg.ac.rs)

[9]Department of Environmental Engineering, Technical University of Denmark, DK-4000 Roskilde, Denmark (jiqi@dtu.dk)

[10]National Measurement Laboratory, Queens Road, Teddington Middlesex TW11 0LY, United Kingdom (ben.russell@npl.co.uk)

Key words: reference material, homogeneity, quality control, mass spectrometry, environmental monitoring

Abstract

There are very few radioactive environmental reference materials (RM) traceable to the International System of Units. Existing radioactive RMs for environmental samples that can be measured by mass spectrometry are even more limited and their characterisation does not always include relevant parameters such as isotopic ratios. This paper focuses on the development of two environmentally relevant candidate RMs, one liquid and one solid, which could be used for routine quality control measurements.

The liquid RM was prepared by spiking seawater sampled from the North Sea, and therefore the matrix is representative of a real environmental sample, while the solid RM was prepared using a synthetic approach by spiking a mixture of silica precursors before a *sol-gel* reaction. The homogeneity, between-bottles and within-bottles, of both RMs was assessed using gamma-ray spectrometry and mass spectrometry. For the liquid RM, the variation among sub-samples was due mainly to the within-bottle variance, and was lower than 1 %, for all the radionuclides tested. For the solid RM, the ^{241}Am content measured with gamma-ray spectrometry revealed a statistically significant variation between-bottles, but was lower than 1 %. The ^{238}U and ^{239}Pu contents, measured by mass spectrometry, showed higher measurement variability (~5 %), with the main contribution coming from within the bottles.

Introduction

Radioactive elements are present in the environment, either naturally or due to anthropogenic activities such as operation of nuclear power plants, mining, weapons testing (in the past) or accidents (Adeola et al., 2023; Nies, 2018; Salbu et al., 2015; Valkovic, 2000). The European Atomic Energy Community (Euratom) provides dose limits for exposure of members of the public to ionising radiation and radionuclides due to unplanned exposure situations (Euratom, 2013). Therefore, in every country, periodic analysis of environmental samples (soils, sediments, waters, plants, etc.) are conducted to ensure that authorised levels are not exceeded.

Common radioactive pollutants can be detected using their emitted radiation. Gamma-ray spectrometry, for example, has been widely used, notably because it is non-destructive (Semkow et al., 2002). However, for

long-lived radionuclides, radiometric techniques are not the most appropriate to detect low levels of contamination (low efficiency of some gamma rays; time-consuming alpha-particle spectrometry). Mass spectrometry techniques, such as accelerator mass spectrometry (AMS) and inductively coupled mass spectrometry (ICP-MS), possess high sensitivity and low detection limits (Ben Yaala et al., 2019; Zheng et al., 2022), and can also provide the quantification of different isotopes of the same element, provided their half-lives are long enough, which may not be easily achieved with common radiometric techniques. Mass spectrometry can also be used to derive isotopic ratios (Lariviere et al., 2006). This is especially interesting for uranium isotopes, where a deviation from natural isotopic ratios can reveal anthropogenic contamination of the environment (Barrado et al., 2024; Boulyga and Becker, 2001; Richter et al., 1999).

With mass spectrometry, as with any analytical procedure, it is crucial to verify and ensure the accuracy of the measurements. This can be done by using calibrated instruments and by regularly checking the instrument response with relevant standards. When environmental samples are measured, the influence of the sample matrix adds an additional difficulty. The sample can be liquid, solid or particulate, for example, with chemical species that might interfere during the measurement and introduce additional bias, commonly called “matrix effects” (Kadis, 2002). Therefore, “pure” radioactivity standards may not suffice to ensure the accuracy of an analytical procedure. Environmental reference materials (RM), whose matrices are similar to those of natural samples such as ground water, seawater, soil, sand, sediments, or food, are often used. The characteristics of such reference materials should ideally have been quantified with metrological techniques and be traceable to the International System of Units (SI). For radioactive measurands, however, the variety of environmental RMs is low, and those measurable by mass spectrometry are even more limited (Inn et al., 2016). Furthermore, their characterisation does not always include several elements or relevant parameters such as isotopic ratios (Brand et al., 2014; Vogl et al., 2013).

Environmental RMs can be produced using two approaches: using native samples or by adding a known quantity of radionuclides in a blank matrix as a “spike” (Jakopič et al., 2013). Native samples have been collected, for example, from Chernobyl (Llauradó et al., 2001) or Fukushima (Unno et al., 2014) areas, industrial sites (Shakhashiro et al., 2012), and from non-contaminated areas for lower radionuclide contents (Pham et al., 2014). These have the advantage of being the most representative of real environmental samples. However, the exact content of radionuclides can be obtained only from measurements by trusted laboratories. Spiked RMs are usually less representative of environmental samples but tend to be more ideal with respect to the accuracy level of spiking and straight-forward traceability (Jerome et al., 1994; Lourenço et al., 2014; Peng and Wang, 2013).

An important part of RM production is assessing homogeneity, as described in a standard on their production (ISO 33405, 2024). This assessment assures that the distributed RM bottles are equivalent, within uncertainties, and that if sub-sampling is performed the differences among sub-samples are taken into account in the uncertainty evaluation of the RM’s characteristics.

Herein, two environmental RMs were produced, one liquid using a seawater matrix and one solid using a synthetic silica matrix, each containing a mix of ^{234}U, ^{235}U, ^{236}U, ^{237}Np ^{238}U, ^{239}Pu, ^{240}Pu and ^{241}Am. A spiking approach was chosen to allow a comparison between the values obtained from measurement and from spiking. These RMs will be used, as part of the European project MetroPOEM, in two interlaboratory comparisons, each involving about 15 participants, to evaluate analytical methods. This article describes the production methods for both RMs and the homogeneity assessment of three radionuclides, ^{241}Am, ^{238}U and ^{239}Pu. To evaluate the homogeneity of both RMs, the variation of the content of ^{238}U, ^{239}Pu and ^{241}Am over several sub-samples was measured using gamma-ray spectrometry (non-destructive) and mass spectrometry (destructive). Both within- and between-bottle homogeneity were assessed, to ensure that each RM bottle contained the same value for each property, within uncertainties.

Materials and methods

Materials

Ethanol (EtOH, VWR, 96 %), tetraethyl orthosilicate (TEOS, Sigma-Aldrich, > 99 %), triethoxyoctylsilane (TOS, Sigma-Aldrich 97 %), hydrofluoric acid (HF, Merck, 40 %), hydrochloric acid (HCl, SCP Science, 32 – 35 %), nitric acid Normatom® (HNO_3, VWR, 68 %), hydrogen peroxide (H_2O_2, Merck, 30 %), ascorbic acid (Sigma-Aldrich, 99.7 - 100.5 %) and sulfamic acid (Labosi, 99.5 %) were used as received. 3 mol/L HNO_3, 2 % HNO_3, 0.02 mol/L, 3 % H_2O_2, 0.002 mol/L ascorbic acid, and 0.005 mol/L sulfamic acid were obtained by diluting the concentrated solution with ultrapure water.

All vials and reaction vessels were cleaned by immersing in 2 % HNO_3 for 24 h, followed by rinsing with ultrapure water and drying in a ventilated oven at 70 °C.

Six starting radioactive solutions were used: a solution of ^{241}Am, two solutions of $^{239/240}$Pu, and a solution of ^{234}U, ^{235}U, ^{236}U and ^{238}U were supplied by the *Commissariat à l'Energie Atomique* (France, CEA). A solution of ^{237}Np and a solution of ^{234}U, ^{235}U, ^{236}U and ^{238}U were supplied by the National Physics Laboratory (UK, NPL).

Production of the liquid RM

Approximately 250 L of seawater were sampled by Helmholtz-Zentrum Hereon in the North Sea mid-May 2023. The seawater was filtered directly onboard during the sampling using cleaned PALL Acropak filters according to the Geotraces Cookbook (Cutter, n.d.). The prefilter pore diameter was 0.8 µm, with a final filtering diameter of 0.2 µm. Afterwards, the seawater was stabilised with the necessary amount of acid to reach 0.1 mol/L of HNO_3, and sterilised by delivering a dose of 25 kGy using a ^{60}Co irradiator. The raw seawater was measured by five partners (Technical University of Denmark, *Eidgenössische Technische Hochschule Zürich*, *Physikalisch-Technische Bundesanstalt*, CEA and *Vinča Institut za Nuklearne Nauke Serbia*) to determine the initial mass fractions of the radionuclides of interest. The details of this study are given in Appendix A.

For the spiking procedure, the four starting radionuclide solutions (weighed accurately at CMI) were first mixed and diluted to yield around 100 g of a multi-radionuclide (RN) spiking mixture containing ^{234}U, ^{235}U, ^{236}U, ^{238}U, ^{239}Pu, ^{240}Pu, ^{241}Am, and ^{237}Np. Then, 98 g of the mixture were mixed with ~40 L of seawater in a closed container for two weeks at 20 °C; 80 samples of 0.5 L each were aliquoted (Figure S1). The samples were labelled with increasing filling order, to identify any possible bias between the top and bottom of the container, which could be caused by sedimentation of particulate matter remaining in the seawater.

The minimal sample size for analysis was chosen to be 5 mL, based on the approximate radionuclide content, to ensure that the participants could measure the characteristics of the liquid RM.

Production of the solid RM

The details of the formulation of the solid RM are given in Appendix B. For the preparation of the batch of solid RM, the four starting radionuclide solutions were mixed and diluted to yield 100 g of a multi-RN spiking mixture containing ^{234}U, ^{235}U, ^{236}U, ^{238}U, ^{239}Pu, ^{240}Pu, ^{241}Am, and ^{237}Np. The solutions were weighed accurately using the pycnometer method, at the CEA. After mixing for 24 h, 98 g, were diluted to around 3 kg with 3 mol/L nitric acid and left to homogenise for 24 h with a magnetic stirrer at ambient conditions in a closed flask. The entire solution was transferred to the reaction medium, with 15 kg (72 mol) of TEOS, 6.8 kg (25 mol) of TOS, 4.8 kg of EtOH, and 0.9 kg of 3 mol/L HNO_3, and stirred for five days. The mixture was then separated into nine trays, using a hand pump. The weight of the liquid transferred was measured using a Mettler Toledo KB60 balance (range 60 kg, resolution 1 g). The trays were left at room temperature for 8 days until gelation occurred. They were then placed in an oven at 70 °C for five days, followed by 4 days at 100 °C, until the mass of the solid did not vary. The resulting solid was milled for 7 h at 100 rpm (9 kg of solid divided among 4 mill jars). A total of 82 bottles of solid RM containing about 100 g of material each were produced (Figure S1). The samples were labelled with increasing filling order to identify any possible bias among the different trays in which the reaction mixture was transferred.

Scanning electron microscopy

Scanning Electron Microscopy (SEM) images were obtained from both spiked and unspiked silicate powders in their supplied form. All particles were transferred onto SEM stubs, which are made of aluminium and prepared with a layer of carbon tape. The SEM used for imaging was a Philips XL30 equipped with an Energy Dispersive X-ray Spectroscopy (EDS) system featuring a Silicon Drift Detector (SDD), both sourced from remX GmbH in Bruchsal, Germany (Leifermann et al., 2023). To mitigate image artefacts caused by the silicate's low electrical conductivity, imaging was performed in Backscattered Electron (BSE) mode.

Gamma-ray spectrometry for homogeneity studies

For the liquid RM, one 50 mL aliquot and five 15 mL aliquots were taken from each of five bottles, labelled, and measured as is (Figure S2). For the solid RM, three to five 7 g aliquots and five 0.7 g aliquots were taken from each of eight or five bottles (Figure S3). The solid material was placed in cylindrical boxes (4 cm diameter for the 7 g aliquots, 1.6 cm diameter for the 0.7 g aliquots, 0.8 cm thickness), and packed tightly.

An HPGe detector (Canberra) was used to measure the ^{241}Am content and its variation among the different sub-samples. For the liquid RM, the 50 mL samples were measured 10 cm from the detector for ~20 h, while the 15 mL samples were measured in direct contact with the detector for a duration ranging from 3 h to 18 h. For the solid RM, the 7 g samples were measured 10 cm from the detector and the 0.7 g samples were measured in contact with the detector, for ~ 20 h.

Attenuation measurements were performed using a ^{152}Eu source and a ^{133}Ba source with lead collimators. Attenuation measurements lasted between 3 and 15 h and were performed for each solid sub-sample. The linear absorption coefficient at 59.54 keV was obtained from the fit of the experimental curve and was used to correct the data obtained from the measurement of the 59.54 keV ^{241}Am peak (Figure S4). The linear absorption coefficients of all 0.7 g sub-samples were similar at about 0.15 cm^{-1}.

The uncertainty budgets of the measurement of a single sub-sample of the liquid and solid RM are presented in Table S1.

Mass spectrometry for homogeneity assessment

For the liquid RM, three aliquots of 5 g were sampled from each of three bottles (Figure S2). Each sample was spiked with a known quantity of ^{235}U (U970) and ^{242}Pu (IRMM-049e) using the isotope dilution technique (Quemet et al., 2024). After spiking, samples were mixed overnight and subsequently evaporated to dryness on a hot plate at 150 °C. Following evaporation, 32-35 wt% hydrochloric acid was added to each sample and digestion was carried out overnight at 80 °C before the sample was evaporated to dryness again, at 150 °C on a hot plate. A 0.5 mL mixture of 6 mol/L HNO_3 and 3 % H_2O_2 was added to each sample and allowed to react for 2 h prior to loading onto UTEVA resin columns (Triskem International).

Pu was eluted using a mixture of 2 mol/L HNO_3, 0.002 mol/L ascorbic acid, and 0.005 mol/L sulfamic acid, while U was eluted using 0.02 mol/L HNO_3. Both Pu and U fractions were evaporated to dryness. 200 µL of 30 % H_2O_2 was then added to both fractions to remove the organic components before evaporation to dryness. The U fraction was diluted to a final concentration of 100 ng/g in 2 % HNO_3. All samples were analysed using a Neptune Plus (Thermo Fisher) multi-collector ICP-MS. IRMM-186 was used as a standard to correct for mass bias, and measurements were performed using the standard bracketing method (Albarède et al., 2004).

For the solid RM, four 0.5 g aliquots and one 2 g aliquot were sampled from each of five bottles (Figure S3). The solid powder was weighed in an aluminium crucible then placed in a ventilated oven at 105 °C for 16 hours. The samples were then placed in a desiccator for 30 min to cool down without absorbing moisture and then weighed to determine their dry mass. The crucibles were then placed in a furnace at 550 °C for 16 hours to remove the organic component. The solids were transferred to PTFE beakers and, for the 0.5 g samples, 1.5 mL of 68 % HNO_3 and 1.5 mL of 40 % HF were added; for the 2 g samples, 7 g of 68 % HNO_3 and 7 g of 40 % HF were used. The beakers were placed on a hot plate at 200 °C for 30 min, when the solid was completely dissolved. Then, the acid mixture was evaporated in the same conditions and the remnant was dissolved again in 2 % HNO_3 three times and evaporated to dryness each time.

Prior to the measurements, 1 mL of 2 % HNO_3 was added to each sample and mixed overnight. Subsequently, 0.5 g samples were diluted using a dilution factor of 20, and the 2 g samples a dilution factor of 36-40. Bi-209 (SPEX CertiPrep) was added to all samples as an internal standard to correct for matrix effects. Analyses were performed using a X7 Series II (ThermoFisher) quadrupole ICP-MS to determine the concentrations of U and Pu. Three separate calibrations with ^{238}U (SPEX CertiPrep) were used for the quantification of each element. For each calibration curve, the same set of samples were analysed on the same day to ensure internal consistency across the measurements. In total, the procedure was repeated over three days – each day using a different calibration curve with the same set of samples.

For the silica samples, the uncertainty came mainly from uncertainty of the calibration curve and from the peak intensity counting statistics, while for the seawater sample, uncertainty propagation of all terms of the isotope dilution equation using Kragten's method was applied (Kragten, 1994). Detailed uncertainty budgets for the mass spectrometry measurements are presented in Table S2 and Table S3.

Results and Discussion

Liquid candidate RM

Preparation of the liquid RM

In order to choose the spiking level of the liquid RM, the raw seawater was first measured in five chosen laboratories (DTU, ETZH, PTB, CEA, and VINS). Mass spectrometry was used by four laboratories; the VINS used gamma-ray spectrometry; experimental details are given in Appendix A.

Participants reported mainly the mass fraction of ^{238}U. Other mass fractions and isotope ratios were measured by some of the participants but are not reported in this work. For example, the $^{236}U/^{238}U$ isotope ratio and the mass fractions of Pu isotopes were measured with AMS, but could not be measured with other mass spectrometry methods. For the AMS measurement of ^{238}U, neither the instrumental settings nor the amount of spike added were optimized for this isotope, resulting in higher uncertainties. The activities of uranium and plutonium isotopes were below the detection threshold of gamma-ray spectrometry and results were not considered in the calculation of averages. The participants did not detect any ^{241}Am or ^{237}Np, regardless of measurement technique.

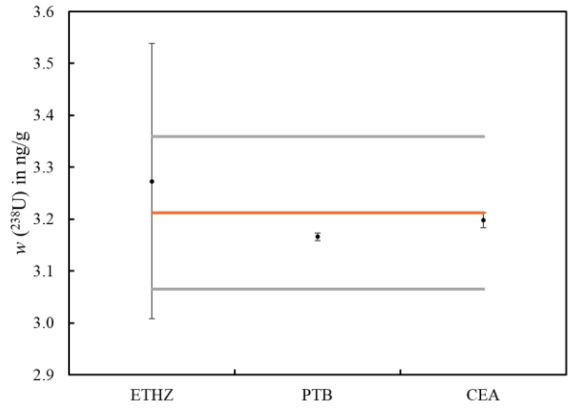

Figure 1. Results of mass fraction for ^{238}U in raw seawater, performed by three partner laboratories, using mass spectrometry. The orange line represents the average of the three values, and the grey lines are the mean value plus/minus the standard deviation among the three values. All bars correspond to the combined standard uncertainty (k = 1) on each result.

From the average of three sets of mass spectrometry measurements, the ^{238}U mass fraction was determined to be about 3 ng/g (Figure 1). Although the measurements from the participants do not agree with one another at k = 1, the value and ranges on uncertainties were in agreement with reported data for

environmental seawater samples, with values between 3.0 and 3.6 ng/g for the ^{238}U mass fraction, considering that the sampled seawater was diluted on the ship to acidify it (Chen et al., 1986; Owens et al., 2011). These values were taken into account when the material was spiked with radionuclide solutions to yield the appropriate radionuclide content of the liquid candidate RM (Table 1). The targeted uncertainty for the characteristics of this liquid RM was between 1 % and 5 %.

Table 1. Characteristics of the liquid RM after spiking.

Radionuclide	Natural U	^{239}Pu	^{240}Pu	^{241}Am	^{237}Np
Approximate mass fraction in liquid RM, in ng/g	< 60	< 1	< 0.2	< 0.2	< 1

Homogeneity study

Gamma-ray spectrometry and mass spectrometry were used to evaluate the homogeneity of the liquid RM. Even if the liquid RM was mixed thoroughly, the radionuclides could precipitate, either by adsorbing on microparticles sill present in the seawater despite filtration, or by the formation of insoluble Pu particles. Furthermore, radionuclides could adsorb on the walls of the containers, and this adsorption could be different for each RM bottle.

Although the measurements for the 15 mL samples analysed with gamma-ray spectrometry were not repeated, the counting statistics were used an estimate of the repeatability of the measurement. As presented in Table S1, showing the uncertainty budget for each individual measurement, the main contribution to the uncertainty is the counting statistics, which are expected to be relatively consistent across these measurements.

For each 15 mL sub-sample, the signal obtained by gamma-ray spectrometry at 59.54 keV was normalised by the mass of the sample. The relative variation of each measurement to the average of the twenty-five measurements (sub-samples) is shown in Figure 2.

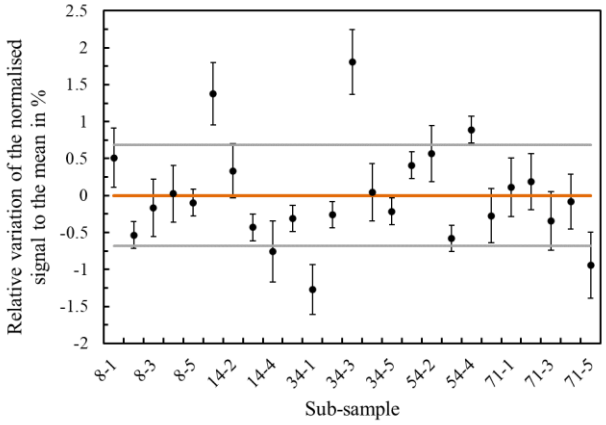

Figure 2. Relative variation of the gamma-ray spectrometer response on ^{241}Am (in cps/s/g) to the average of the results, for the twenty-five sub-samples of 15 mL of the liquid RM. The bars represent the uncertainty of each individual measurement. The orange line represents the average of the values of the sub-samples, and the grey lines represent the standard deviation between the values of the sub-samples.

No outlier result was detected using a Grubbs test (ISO 5725-2, 2022). No outward or downward trend was observed, indicating the absence of any filling order bias.

A one-way analysis of variance (ANOVA) was performed to compare the variance within bottles (five sub-samples per bottle) and among bottles (five bottles) (Table 2). The details of the ANOVA are given in the supplementary information.

Table 2. ANOVA for the ^{241}Am homogeneity study on 15 mL samples.

Variation source	Mean squares	F value	Critical F value (F_{crit}) ($\alpha = 0.05$)	Variance in %
Between-bottle	$1.40 \cdot 10^{-6}$	0.213	2.87	$s_{bb} = 0$ ($s_{bb}^2 < 0$)
Within-bottle	$6.95 \cdot 10^{-6}$			$s_{wb} = 0.7$

The main contribution to the variance came from within the bottles, with $s_{wb} = 0.7$ %. The variance between bottles was negligible, with $s_{bb}^2 < 0$, which agreed with the Fisher test ($F < F_{crit}$). The variance within bottles was of the same order of magnitude as the counting statistics of each individual measurement, which varied from 0.2 % to 0.5 % (Table S1), therefore the counting statistics may contribute to the apparent within-bottle variance. Gamma-ray spectrometry was also used to measure five 50 mL sub-samples, and the results are presented in Figure S5.

Mass spectrometry was used to assess the homogeneity of ^{238}U, whose chemistry is representative of all hexavalent U isotopes in the liquid RM. The uncertainties of the measurements were evaluated independently be to 0.29 % for ^{238}U and 0.19 % for ^{239}Pu. The main contributions to uncertainty came from the spike concentration (see Table S2 for the detailed uncertainty budget), and, therefore, can be used to estimate the repeatability of the measurement.

The results of the ^{238}U and ^{239}Pu measurements are presented in Figure 3 and Figure S6, respectively, with the standard uncertainty presented as bars.

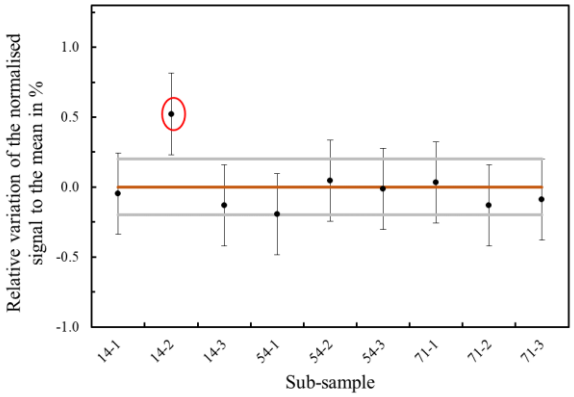

Figure 3. Relative variation of the mass spectrometry measurements of ^{238}U to the average of the results, for the nine sub-samples of 5 mL of the liquid RM. The bars represent the uncertainty of each individual measurement, at $k = 1$. The orange line represents the average of the values of the sub-samples, and the grey lines represent the standard deviation among the values of the sub-samples. The circled point was identified as suspicious.

Sub-sample 14-2 was flagged as suspicious by a Grubbs test (ISO 5725-2, 2022) for ^{238}U; therefore, the sample was removed from the following analyses. No upward or downward trend was observed with the filling order of the bottles.

A one-way analysis of variance (ANOVA) was performed to compare the variance within-bottles (three sub-samples per bottle) and between-bottles (three bottles) (Table 3). The details of the ANOVA performed are given in the supplementary information.

Table 3. ANOVA for the ^{238}U homogeneity study on 5 mL samples.

	Variation source	Mean squares	F value	Critical F value ($\alpha = 0.05$)	Variance in %
^{238}U	Between-bottle	$1.27 \cdot 10^{-4}$	0.08	5.78	$s_{bb} = 0$ ($s_{bb}^2 < 0$)
	Within-bottle	$4.11 \cdot 10^{-3}$			$s_{wb} = 0.1$
^{239}Pu	Between-bottle	$1.19 \cdot 10^{-6}$		5.14	$s_{bb} = 0$ ($s_{bb}^2 < 0$)

	Within-bottle	$4.31 \cdot 10^{-6}$	0.82		$s_{wb} = 0.1$

For both ^{238}U and ^{239}Pu the "bottle" parameter was not significant according to the Fisher test ($F < F_{crit}$). The main contribution to the variance came from within the bottles, with $s_{bb} = 0.1$ % for ^{238}U and ^{239}Pu; $s_{wb} = 0$ % (s_{wb}^2 was negative) in both cases. The variances calculated with ANOVA were very low, on the same order of magnitude as the uncertainty of a single measurement, and were below the requirements for the overall uncertainty of the characteristics of the reference material (1 % to 5 %).

The results of between-bottle variance and within-bottle variance for ^{241}Am measured by gamma-ray spectrometry on 15 mL samples, and for ^{238}U measured with mass spectrometry on 5 mL samples, were similar. In both cases, the between-bottle variance was negligible and the within-bottle variance was comparable to the measurement variation. The value of the variation was below 1 %, which is within requirements for the liquid RM (final uncertainty of 1 % to 5 %). The sample preparation steps for mass spectrometry did not seem to introduce an additional variation on the results. Furthermore, the two different radionuclides did not seem to be distributed differently in the liquid RM; the homogeneity level of the liquid RM seemed to be the same for 5 mL and for 15 mL.

These values for the between-bottle and within-bottle homogeneity are lower than those reported for non-spiked environmental RMs, such as mineral water or seawater. For example, Spasova et al. (2009) reported both between-bottle and within-bottle variances of 2.5 % and Pham et al. (2011) reported a between-bottle variance below 10 %, using radiometric techniques, for ^{234}U and ^{238}U. This difference could either be due to the different measurement techniques, or to a more efficient mixing process.

Solid candidate RM

Preparation of the material

The approach from Harms and Gilligan (2012) was chosen as a starting point to produce a homogeneous material. The other main approach to prepare spiked solid RMs is to add a radioactive solution to a slurry of a real sample such as soil or grass, usually in a volatile solvent, followed by evaporation of the solvent (Lourenço et al., 2014; Sanoit, 1994). With this approach, the radioactivity is expected to be adsorbed on the surface of the particles forming the RM. However, the approach chosen in this work distributes the radionuclides throughout the silica matrix. Furthermore, the sol-gel process enables the mixing of the reagents and the radionuclides together in a liquid phase to ensure homogeneity before the formation of the solid.

In the publication from Harms and Gilligan (2012), a standard uncertainty of 2.5 % was chosen to account for the moisture content. The CEA chose to modify the reaction precursors to reduce the moisture uptake of the resulting silicate matrix from 8 % to around 3 %. The experimental details and results of this optimisation are presented in Appendix B.

Scanning electron microscopic images of the inactive solid and spiked solid RM were taken at Gottfried Wilhelm Leibniz University Hannover (Figure 4). In the BSE mode (see experimental details), heavier elements reflect a greater proportion of the incident electrons due to their higher atomic number and charge density, resulting in increased brightness in the BSE images. Therefore, silicate particles are distinctly visible against the carbon background. The solid material comprised polydisperse particles, ranging from a few µm to around 100 µm.

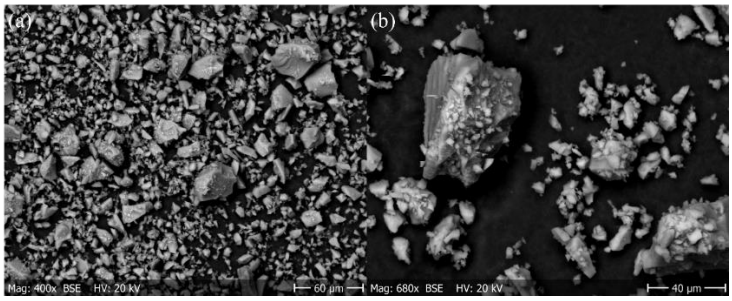

Figure 4. SEM images of the solid RM after calcination magnified 400 times (a) and 680 times (b).

EDS spectra and elemental mappings revealed that the sample components consisted exclusively of silicon, carbon, and oxygen and the corresponding images are shown in Figure S7. This analysis does not permit to detect the radionuclides added by spiking. The O and Si atoms seem uniformly distributed over the particles.

The material was spiked with radionuclide solutions to yield the intended radionuclide content of the solid candidate RM (Table 4). The targeted uncertainty for the characteristics of this solid RM was between 1 % and 5 %.

Table 4. Characteristics of the solid RM after spiking.

Radionuclide	U (slightly enriched)	^{239}Pu	^{240}Pu	^{241}Am	^{237}Np
Approximate mass fraction in solid RM in ng/g	< 50	< 2	< 0.1	< 1	< 1

Homogeneity study

Gamma-ray spectrometry and mass spectrometry were used to evaluate the homogeneity of the solid RM. Even if the radionuclides were mixed with the silica precursors as a liquid, several processes could lead to a non-homogeneous material: silica might first be formed as small nano- or micro-sized nuclei, on which the radionuclides might adsorb and which might precipitate. Furthermore, the speciation of the U, Pu, Am and Np isotopes in an organic medium is unknown, and precipitates might be formed. While previous work (Harms and Gilligan, 2012) did not report a high inhomogeneity (the contribution to uncertainty varied from 0.4 % to 4 %, depending on the radionuclides), the material prepared here comprised different radionuclides (U, Pu, Np), and was prepared from nitric acid and not hydrochloric (see Appendix B for more details on the synthesis).

The 0.7 g samples were measured by gamma-ray spectrometry and the signal of the instrument, normalised by the mass of the sample, was compared for each sample. Even though measurements were not repeated, repeatability could be determined by the uncertainty on each measurement (Table S1). The main contribution to the uncertainty was the attenuation correction, around 1 %. The attenuation measurements were performed on each sub-sample, and an average correction was applied. Therefore, variations among the measurement of sub-samples may come from a difference in attenuation of the emitted gamma rays, resulting from a different packing of the powder in the cylindrical boxes. The estimated uncertainty for the attenuation correction was used as an estimate of the repeatability of the measurement. The results of the variation of each sub-sample from the average of the 40 sub-samples is presented in Figure 5.

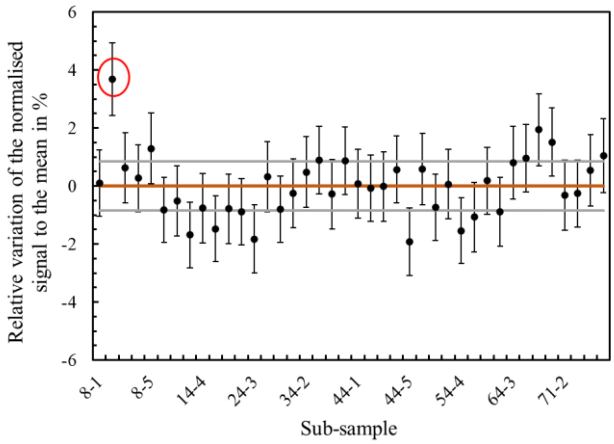

Figure 5. Relative variation of the gamma-ray spectrometer instrument response to ^{241}Am (in cps/s/g) on the average of the results for forty sub-samples of 0.7 g of the solid RM. The bars represent the uncertainty of each measurement, at $k = 1$. The orange line represents the average of the values of the sub-samples, and the grey lines represent the standard deviation of the values of the sub-samples. The circled point was identified as suspicious.

Sample 8-2 was flagged as suspicious by a Grubbs test (ISO 5725-2, 2022), and was removed from subsequent analyses. No upward or downward trend was observed with the filling order, indicating that the variation of composition was random. A one-way analysis of variance (ANOVA) was performed, to compare the variance within-bottles (five sub-samples per bottle) and between-bottles (eight bottles) (Table 5).

Table 5. ANOVA analysis for the ^{241}Am homogeneity study on 0.7 g samples.

Variation source	Mean squares	F value	Critical F value ($\alpha = 0.05$)	Variance in %
Between-bottles	$4.93 \cdot 10^{-3}$	3.51	2.32	$s_{bb} = 0.7$
Within-bottles	$1.41 \cdot 10^{-3}$			$s_{wb} = 0.9$

The between-bottles and within-bottles variances were similar, $s_{bb} = 0.7$ % and $s_{wb} = 0.9$ %, respectively. The parameter "bottle" was statistically significant ($F > F_{crit}$), which means that the variation observed between the bottles cannot be explained by only the variation within the bottles. The uncertainty contribution coming from the attenuation correction of each individual measurement was around 1 %, which certainly contributed to the within-bottle and between-bottle variances. Furthermore, the values of both between-bottle and within-bottle variances are within requirement for the total uncertainty of the characteristics of the solid material (1 % - 5 %). Sub-samples of 7 g of the solid RM were also analysed by gamma-ray spectrometry, and the results are presented in Figure S8.

Mass spectrometry was used to assess the homogeneity of ^{238}U and ^{239}Pu in the solid RM. Contrary to the gamma-ray spectrometry measurements, the solid RM needed to be dissolved (as described in Materials and Methods) before analysis. Each sub-sample was analysed three times, using a different calibration curve. The uncertainty budget of these measurements is presented in Table S3. The main contribution comes from the calibration curve and from the repeatability of the measurements, for ^{238}U, and from the signal intensity of the ^{238}U peak and the repeatability of the measurement for ^{239}Pu.

The results of the measurements of ^{238}U and ^{239}Pu are presented in Figure 6 and Figure S9, respectively, where the average value over the three measurements is plotted for each sub-sample.

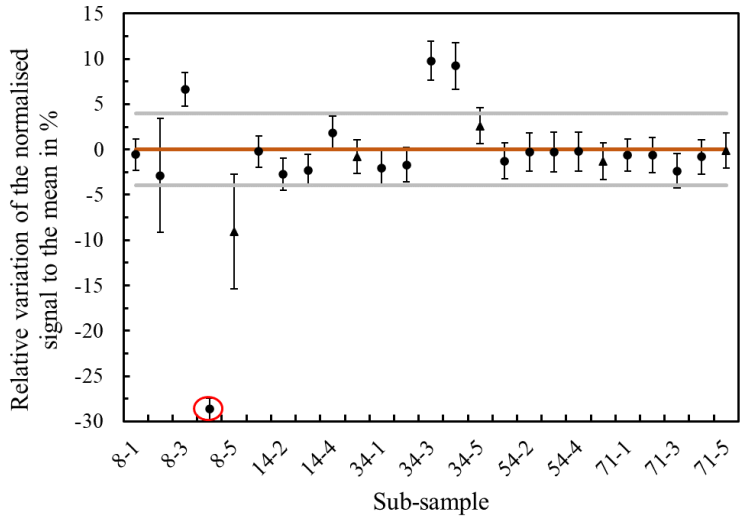

Figure 6. Relative variation of the mass spectrometry measurements to the average of the results, for the twenty-five sub-samples of 0.5 g (dots) and 2 g (triangles) of the solid RM, for ^{238}U. The bars represent the uncertainty of the individual measurements. The orange line represents the average of the values, and the grey lines represent the standard deviation of the values. The point circled was identified as aberrant.

The ^{238}U and ^{239}Pu measurements for sample 8-4 were flagged as aberrant by a Grubbs test (ISO 5725-2, 2022) and were removed from subsequent analyses. This sample probably lost some material during calcination, dissolution of evaporation. No downward or upward trend was observed with the filling order of the bottles. No significant difference was observed between the ^{238}U and ^{239}Pu measurements of the 0.5 g samples and the 2 g samples when an ANOVA was conducted by grouping the data by sample size (Table S4). Therefore, in the following, no distinction is made between 2 g and 0.5 g samples.

The within-bottle homogeneity was assessed using ANOVA for each bottle and considering all three measurements, which gave an indication on the repeatability of measurement (Table S5). The measurement variance among the bottles was from 0.6 % to 4.7 % for ^{238}U and between 2.9 % and 7.8 % for ^{239}Pu. For most bottles, $F > F_{crit}$ (the variance within bottles was statistically significant). This was different from the gamma-ray spectrometry results, where the within-unit variance was lower than the standard uncertainty. Since the amounts of material tested were similar, this was probably due to an additional variability introduced by the sample preparation steps of calcination and dissolution. Furthermore, the uncertainty of the mass spectrometry measurement of a single sub-sample was higher than that of the gamma-ray spectrometry measurement (~ 1.7 % for ^{238}U and ~ 6 % for ^{239}Pu), which could also partly explain the higher variability observed.

To assess the between-bottles homogeneity, the average of all three measurements for each sub-sample were compared using a one-way ANOVA (Table 6).

Table 6. ANOVA for between-bottle homogeneity of ^{238}U and ^{239}Pu concentrations by mass spectrometry, on 0.5 g and 2 g dissolved samples.

Element	Mean squares		F value	F_{crit} ($\alpha = 0.05$)	Variance in %
^{238}U	Between-bottles	2.50	1.43	2.89	s_{bb} = 0.4
	Within-bottles	1.75			s_{wb} = 3.8
^{239}Pu	Between-bottles	$4.60 \cdot 10^{-3}$	1.52	2.89	s_{bb} = 0.9
	Within-bottles	$3.02 \cdot 10^{-3}$			s_{wb} = 6.3

The main contribution to the variance came from within the bottles, calculated as 3.8 % for ^{238}U and 6.3 % for ^{239}Pu, similar to estimations of previous analysis where repeated measurements were taken into account

(for ^{238}U, s_{wb} was between 0 % and 3.2 % and for ^{239}Pu, s_{wb} was between 0 % and 4.9 %, see Table S5). The between-bottle variance was not statistically significant ($F < F_{crit}$) and was calculated to be 0.4 % for ^{238}U and 0.9 % for ^{239}Pu.

These results were different from the gamma-ray spectrometry measurements, where the between-bottle variance was not negligible. With the sample size very similar for both measurements, 0.7 g for gamma-ray spectrometry and 0.5 g for mass spectrometry, this could indicate a different distribution of ^{241}Am compared to ^{238}U and ^{239}Pu in the solid RM. However, it is more likely that any inhomogeneity among bottles was masked by the higher within-bottle variance due to the sample preparation procedure, and the higher variation of the measurement, for the mass spectrometry measurement. The values of the within-bottle variance are close to the targeted total uncertainty for the solid RM (1 % to 5 %), and will be taken into account when establishing the uncertainty of the characteristics of the reference material.

The results for the between-bottle and within-bottle variance were similar to those reported for natural non-spiked soil RM. For example, Shakhashiro et al. (2011) presented a between-bottle variance of around 0.5 % and a within-bottle variance of 2.2 % for ^{234}U and ^{238}U measured by alpha-particle spectrometry for a soil RM, and Larijani et al. (2017) reported a between-bottle variance of around 1 % for ^{238}U measured by gamma-ray spectrometry, for a rock RM.

Conclusion

This work aimed to develop and characterise two environmentally relevant reference materials (RMs) - one liquid (seawater) and one solid (silicate) - containing various radioactive isotopes including ^{238}U, ^{239}Pu, and ^{241}Am.

The liquid RM was created by spiking North Sea seawater with radioactive solutions and bottled in 80 individual samples. Homogeneity was assessed at three different scales using gamma-ray spectrometry for ^{241}Am and mass spectrometry for ^{238}U and ^{239}Pu, with sample preparation steps for the latter. ANOVA of the liquid RM showed that, for the three radionuclides, the main contribution to variance came from within the bottles, while the variance among bottles was negligible. The within-bottle variance was lower than 1 %, meeting the requirements for the uncertainty of the liquid RM. The sample preparation (removal of the seawater matrix and separation of U and Pu) did not seem to have an influence on the variance of the samples; all radionuclides measured are expected to be distributed in a similar fashion.

The solid RM was synthesised using a sol-gel process with silica precursors, resulting in a material with radioactivity incorporated within the silicate matrix. The material comprised particles from around 1 µm to 100 µm. Homogeneity was studied at three different levels using gamma-ray spectrometry for ^{241}Am and mass spectrometry for ^{238}U and ^{239}Pu, on dissolved samples for the latter. ANOVA for 0.7 g samples showed that both between-bottle and within-bottle variances were similar and below 1 %. However, the between-bottle variance was statistically significant ($F > F_{crit}$). No upward or downward trend was observed with the filling order, indicating a random variation of composition. Mass spectrometry results on dissolved samples showed measurement variance ranging from 0.6 % to about 5 % for ^{238}U, and from 3 % to about 8 % for ^{239}Pu. Within-bottle variance was statistically significant for most bottles, and between-bottle variance was not statistically significant by mass spectrometry measurement for any of the radionuclides. The higher within-bottle variance by mass spectrometry compared to gamma-ray spectrometry was likely due to additional variability introduced by sample preparation (calcination and dissolution).

The between-bottle and within-bottle variance will be taken into account in the uncertainty of the measurands, as recommended in ISO standards. The homogeneity of both RMs was deemed suitable for their intended use as reference materials for mass spectrometry measurements of environmental radioactive samples.

Acknowledgements

The authors would like to thank Daniel Pröfrock from Helmholtz-Zentrum Hereon, for sampling the seawater that was used as a matrix for the liquid RM.

The project (21GRD09 MetroPOEM) has received funding from the European Partnership on Metrology, co-financed by the European Union's Horizon Europe Research and Innovation Programme and by the Participating States. Funder name: European Partnership on Metrology. Funder ID: 10.13039/100019599. Grant number: 21GRD09 MetroPOEM

References

Adeola, A.O., Iwuozor, K.O., Akpomie, K.G., Adegoke, K.A., Oyedotun, K.O., Ighalo, J.O., Amaku, J.F., Olisah, C., Conradie, J., 2023. Advances in the management of radioactive wastes and radionuclide contamination in environmental compartments: a review. Environ. Geochem. Health 45, 2663–2689. https://doi.org/10.1007/s10653-022-01378-7

Albarède, F., Telouk, P., Blichert-Toft, J., Boyet, M., Agranier, A., Nelson, B., 2004. Precise and accurate isotopic measurements using multiple-collector ICPMS1. Geochim. Cosmochim. Acta 68, 2725–2744. https://doi.org/10.1016/j.gca.2003.11.024

Barrado, A.I., Jimenez, F., Conde, E., Hasözbek, A., Fernandez, M., Escareño, E., Cobo, J.M., 2024. Determination of long half-life radioisotopes by mass spectrometry techniques in NORM materials. Radiat. Phys. Chem. 224, 112013. https://doi.org/10.1016/j.radphyschem.2024.112013

Ben Yaala, H., Fniter, R., Foucher, D., Clarisse, O., 2019. Direct analysis of radium-226 in sediment by ICP-MS: an analytical challenge? J. Anal. At. Spectrom. 34, 1597–1605. https://doi.org/10.1039/C9JA00156E

Boulyga, S.F., Becker, J.S., 2001. Determination of uranium isotopic composition and 236U content of soil samples and hot particles using inductively coupled plasma mass spectrometry. Anal. Bioanal. Chem. 370, 612–617. https://doi.org/10.1007/s002160100838

Brand, W.A., Coplen, T.B., Vogl, J., Rosner, M., Prohaska, T., 2014. Assessment of international reference materials for isotope-ratio analysis (IUPAC Technical Report). Pure Appl. Chem. 86, 425–467. https://doi.org/10.1515/pac-2013-1023

Chen, J.H., Lawrence Edwards, R., Wasserburg, G.J., 1986. 238U, 234U and 232Th in seawater. Earth Planet. Sci. Lett. 80, 241–251. https://doi.org/10.1016/0012-821X(86)90108-1

Cutter, G., n.d. Sampling and Sample-handling Protocols for GEOTRACES Cruises.

Euratom, 2013. Council Directive 2013/59/Euratom of 5 December 2013 laying down basic safety standards for protection against the dangers arising from exposure to ionising radiation, and repealing Directives 89/618/Euratom, 90/641/Euratom, 96/29/Euratom, 97/43/Euratom and 2003/122/Euratom.

Harms, A., Gilligan, C., 2012. Development of synthetic environmental radioactivity reference materials. Appl. Radiat. Isot., Proceedings of the 18th International Conference on Radionuclide Metrology and its Applications 70, 1940–1943. https://doi.org/10.1016/j.apradiso.2012.02.055

Inn, K.G.W., LaMont, S., Jerome, S., Essex, R., Johnson, C.M., Morrison, J., Frechou, C., Branger, T., Dion, H., 2016. Roadmap for radioanalytical reference and performance evaluation materials for current and emerging issues. J. Radioanal. Nucl. Chem. 307, 2529–2538. https://doi.org/10.1007/s10967-016-4694-8

ISO 5725-2, 2022. Accuracy (trueness and precision) of measurement methods and results — Part 2: Basic method for the determination of repeatability and reproducibility of a standard measurement method.

ISO 33405, 2024. Reference materials - Guidance for characterization and assessment of homogeneity and stability.

Jakopič, R., Sturm, M., Kraiem, M., Richter, S., Aregbe, Y., 2013. Certified reference materials and reference methods for nuclear safeguards and security. J. Environ. Radioact. 125, 17–22. https://doi.org/10.1016/j.jenvrad.2013.02.013

Jerome, S.M., Woods, M.J., de Felice, P., Pona, C., de Sanoit, J., Dersch, R., 1994. Development of a range of γ-ray emitting radioactive spiked reference materials for environmental monitoring — Part I. Nucl. Instrum. Methods Phys. Res. Sect. Accel. Spectrometers Detect. Assoc. Equip. 339, 55–60. https://doi.org/10.1016/0168-9002(94)91778-7

Kadis, R., 2002. Analytical procedure in terms of measurement (quality) assurance. Accreditation Qual. Assur. 7, 294–298. https://doi.org/10.1007/s00769-002-0484-9

Kragten, J., 1994. Tutorial review. Calculating standard deviations and confidence intervals with a universally applicable spreadsheet technique. The Analyst 119, 2161. https://doi.org/10.1039/an9941902161

Larijani, C., Pearce, A.K., Regan, P.H., Russell, B.C., Jerome, S.M., Crespo, M.T., De Felice, P., Lutter, G., Maringer, F., Mazánová, M., 2017. Reference materials produced for a European metrological research project focussing on measurements of NORM. Appl. Radiat. Isot. 126, 279–284. https://doi.org/10.1016/j.apradiso.2017.02.007

Lariviere, D., Taylor, V.F., Evans, R.D., Cornett, R.J., 2006. Radionuclide determination in environmental samples by inductively coupled plasma mass spectrometry. Spectrochim. Acta Part B At. Spectrosc. 61, 877–904. https://doi.org/10.1016/j.sab.2006.07.004

Leifermann, L., Weiss, M., Chyzhevskyi, I., Dubchak, S., Hanemann, P., Raiwa, M., Schulz, W., Steinhauser, G., Weissenborn, T., Walther, C., 2023. Localisation, isolation and leaching of single hot particles from various environmental matrices in the vicinity of the Chernobyl nuclear power plant. Environ. Radiochem. Anal. VII 357, 0. https://doi.org/10.1039/9781837670758-00001

Llauradó, M., Torres, J.M., Tent, J., Sahuquillo, A., Muntau, H., Rauret, G., 2001. Preparation of a soil reference material for the determination of radionuclides. Anal. Chim. Acta 445, 99–106. https://doi.org/10.1016/S0003-2670(01)01245-4

Lourenço, V., Ferreux, L., Lacour, D., Le Garrérès, I., Morelli, S., 2014. Preparation of spiked grass for use as an environmental radioactivity reference material. Appl. Radiat. Isot. 87, 456–460. https://doi.org/10.1016/j.apradiso.2013.11.034

Nies, H., 2018. Pollution with Radioactive Substances, in: Salomon, M., Markus, T. (Eds.), Handbook on Marine Environment Protection : Science, Impacts and Sustainable Management. Springer International Publishing, Cham, pp. 413–427. https://doi.org/10.1007/978-3-319-60156-4_21

Owens, S.A., Buesseler, K.O., Sims, K.W.W., 2011. Re-evaluating the 238U-salinity relationship in seawater: Implications for the 238U–234Th disequilibrium method. Mar. Chem. 127, 31–39. https://doi.org/10.1016/j.marchem.2011.07.005

Peng, E.-C., Wang, J.-J., 2013. A study of production of radioactive environmental reference materials used for proficiency testing program in Taiwan. Appl. Radiat. Isot. 81, 14–20. https://doi.org/10.1016/j.apradiso.2013.03.041

Pham, M.K., Betti, M., Povinec, P.P., Benmansour, M., Bünger, V., Drefvelin, J., Engeler, C., Flemal, J.M., Gascó, C., Guillevic, J., Gurriaran, R., Groening, M., Happel, J.D., Herrmann, J., Klemola, S., Kloster, M., Kanisch, G., Leonard, K., Long, S., Nielsen, S., Oh, J.-S., Rieth, P.U., Östergren, I., Pettersson, H., Pinhao, N., Pujol, L., Sato, K., Schikowski, J., Varga, Z., Vartti, V.P., Zheng, J., 2011. A certified reference material for radionuclides in the water sample from Irish Sea (IAEA-443). J. Radioanal. Nucl. Chem. 288, 603–611. https://doi.org/10.1007/s10967-010-0976-8

Quemet, A., Hubert, A., Gourgiotis, A., Sánchez Hernández, A.M., Crozet, M., Bailly, G., Dobney, A., Duhamel, G., Hiess, J., Repinc, U., Mialle, S., Boulet, B., Escoube, R., Bouvier-Capely, C., Pointurier, F., Picart, S., 2024. An isotope dilution mass spectrometry overview: tips and

applications for the measurement of radionuclides. J. Anal. At. Spectrom. 39, 1665–1699. https://doi.org/10.1039/D4JA00029C

Richter, S., Alonso, A., De Bolle, W., Wellum, R., Taylor, P.D.P., 1999. Isotopic “fingerprints” for natural uranium ore samples. Int. J. Mass Spectrom. 193, 9–14. https://doi.org/10.1016/S1387-3806(99)00102-5

Salbu, B., Skipperud, L., Lind, O.C., 2015. Sources Contributing to Radionuclides in the Environment: With Focus on Radioactive Particles, in: Walther, C., Gupta, D.K. (Eds.), Radionuclides in the Environment: Influence of Chemical Speciation and Plant Uptake on Radionuclide Migration. Springer International Publishing, Cham, pp. 1–36. https://doi.org/10.1007/978-3-319-22171-7_1

Sanoit, J.D., 1994. Silica Spiked with Mixed y-Ray Standards for Use as Environmental Reference Material. ract 65, 249–258. https://doi.org/10.1524/ract.1994.65.4.249

Semkow, T.M., Parekh, P.P., Schwenker, C.D., Khan, A.J., Bari, A., Colaresi, J.F., Tench, O.K., David, G., Guryn, W., 2002. Low-background gamma spectrometry for environmental radioactivity. Appl. Radiat. Isot. 57, 213–223. https://doi.org/10.1016/S0969-8043(02)00085-4

Shakhashiro, A., Sansone, U., Wershofen, H., Bollhöfer, A., Kim, C.K., Kim, C.S., Kis-Benedek, G., Korun, M., Moune, M., Lee, S.H., Tarjan, S., Al-Masri, M.S., 2011. The new IAEA reference material: IAEA-434 technologically enhanced naturally occurring radioactive materials (TENORM) in phosphogypsum. Appl. Radiat. Isot. 69, 231–236. https://doi.org/10.1016/j.apradiso.2010.09.002

Spasova, Y., Benedik, L., Vasile, M., Beyermann, M., Wätjen, U., Pommé, S., 2009. 234U and 238U in mineral water: reference value and uncertainty evaluation in the frame of an interlaboratory comparison. J. Radioanal. Nucl. Chem. 281, 113–117. https://doi.org/10.1007/s10967-009-0069-8

Unno, Y., Hachinohe, M., Hamamatsu, S., Todoriki, S., Yunoki, A., Miura, T., 2014. Characterization of brown rice as a certified reference material for Fukushima accident-related radioactivity measurements. Appl. Radiat. Isot. 87, 485–488. https://doi.org/10.1016/j.apradiso.2013.11.036

Valkovic, V., 2000. Radioactivity in the Environment: Physicochemical aspects and applications. Elsevier.

Vogl, J., Rosner, M., Pritzkow, W., 2013. The need for new isotope reference materials. Anal. Bioanal. Chem. 405, 2763–2770. https://doi.org/10.1007/s00216-012-6605-3

Zheng, J., Sahoo, S.K., Aono, T., 2022. Recent progress on mass spectrometric analysis of artificial radionuclides in environmental samples collected in Japan. Nucl. Anal. 1, 100025. https://doi.org/10.1016/j.nucana.2022.100025